Dual Electroluminescence from a Single-Component Light-Emitting Electrochemical Cell, Based on Water-Soluble Conjugated Polymer

Zhen Gu,[1] Qun-Dong Shen,[1] Juan Zhang,[1] Chang-Zheng Yang,[1] Yong-Jun Bao[2]

[1]*Department of Polymer Science & Engineering and Key Laboratory of Mesoscopic Chemistry of MOE, College of Chemistry & Chemical Engineering, Nanjing University, Nanjing 210093, People's Republic of China*
[2]*National Laboratory of Solid State Microstructures, Nanjing University, Nanjing 210093, People's Republic of China*

Received 10 April 2005; accepted 23 June 2005
DOI 10.1002/app.22510
Published online in Wiley InterScience (www.interscience.wiley.com).

ABSTRACT: Poly [[2-methoxy-5-(3-sulfonatopropoxy)-1, 4-phenylene]-1, 2-ethenediyl] (MPS-PPV) was an anionic water-soluble conjugated polymer. A novel single-component light-emitting electrochemical cell (LEC) with an indium tin oxide/MPS-PPV/aluminum sandwich structure has been successfully fabricated. MPS-PPV serves as both luminescent material and ionic conductor in the active layer. Electroluminescence can be observed under both forward and reverse bias with emission maxima at about 520 nm (green light). In particular, the device has a low turn-on voltage of about +3V and −4V, and can sustain long-term operations without much loss of efficiency at ambient conditions. © 2006 Wiley Periodicals, Inc. J Appl Polym Sci 100: 2930–2936, 2006

Key words: MPS-PPV; water-soluble polymer; conjugated polymer; luminescence; single-component light-emitting electrochemical cell

INTRODUCTION

Polymer light-emitting diodes (LEDs) have attracted much attention for their application in large-area thin-film displays.[1] For a single-layer LED device formed by sandwiching the semiconducting conjugated polymers between two electrodes, the electroluminescence (EL) originates from radiative decay of singlet excitations generated through recombination of electronic carriers within the active polymer layer. Luminescent polymers such as poly(*p*-phenylene vinylene)s (PPVs) and its derivatives have low electron affinity, which indicates that the ability of electron injection from cathodes is rather worse. Therefore, the emission under reverse bias is usually much weaker than the one under forward bias, and a high operation voltage is required to overcome the carrier injection barrier.

Pei et al. reported a light-emitting electrochemical cell (LEC)[2,3] using a ternary mixture of conjugated polymer, lithium salt, and poly(ethylene oxide) (PEO) as the active layer. Involvement of ionic transport species in the luminescent layer reduces the contact barrier of electrode and polymer.[4,5] LECs exhibit many unique light-emitting behaviors different from conventional LEDs, i.e., the low turn-on voltage close to band gap of PPV, high electroluminescent efficiency, and dual emission under both forward and reverse bias.[6–11] Nevertheless, LECs undergo several shortcomings like poor compatibility between nonpolar semiconducting polymer and polyelectrolyte (PEO and salt), and slow response speed in the range of second. Attempts to obtain a better performance of LECs include usage of binary mixtures either by chemical attachment of oligo(ethylene oxide) side chains onto the backbone of conjugated polymer to improve the phases miscibility of the blends [12–14] or immobilizing anionic species onto polyurethane with PEO as soft segments[15]. In the latter case, the response time of device drastically reduces with respect to bi-ionic transport-based LECs.

In the present study, we investigated a novel single-component LEC with an active layer of poly [[2-methoxy-5-(3-sulfonatopropoxy)-1,4-phenylene]-1,2-ethenediyl] (MPS-PPV, Scheme 1) as both luminescent material and ionic conductor. MPS-PPV is one of the water-soluble conjugated polymers that is shown to be promising candidates for biosensor applications.[16–21] We will demonstrate that LEC with the indium tin oxide (ITO)/MPS-PPV/aluminum structure realizes the complete phase miscibility between the electronic and ionic conductors by anchoring the anionic sulfonate groups to conjugated chain. Since the active layer is homogeneous and maintains its original morphology over a long shelf life, which is unavailable for

Correspondence to: Q.-D. Shen (qdshen@nju.edu.cn).
Contract grant sponsor: National Natural Science Foundation of China; contract grant number: 50228304.

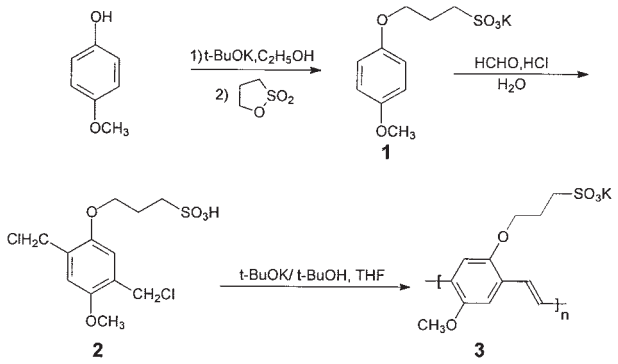

Scheme 1 A brief synthetic route to the MPS-PPV.

binary or ternary composite layer, the devices can be fabricated in batches without obvious difference of composition and keep their original properties to the utmost extent. Meanwhile, the unique behavior of MPS-PPV makes it more suitable in fabrication of high-resolution planar displaying devices via inkjet printing technology developed for water-based ink of the conducting polymer.[22,23] We will show that our device is conspicuously stable under ambient condition and exhibits distinguishable electroluminescent behavior.

EXPERIMENTAL

Materials

Anhydrous toluene and tetrahydrofuran (THF) were obtained by distillation over sodium/diphenyl ketone. Commercial *tert*-butyl alcohol was dried by refluxing with sodium until about two-thirds of the metal was dissolved, and then distilled. 1,3-Propanesultone and potassium *tert*-butoxide from Aldrich were used as received. All other commercial reagent-grade solvents and chemicals were used without further purification.

Characterization

IR spectra were recorded on a Bruker IFS66V vacuum Fourier-transfer spectrometer. ^{1}H NMR spectra were collected on a Bruker DPX300 spectrometer. Gel permeation chromatography (GPC) analysis was measured on an Agilent 1100 series HPLC system equipped with Water's analytical aqueous GPC columns, using poly(ethylene oxide) as standard and 0.1*M* $NaNO_3$ aqueous solution mixed with 20% methanol as eluent. Thermogravimetric analysis (TGA) was conducted on a TA Instrument 2100 system with a TGA 2950 thermogravimetric analyzer under a heating rate of 20°C/min and a nitrogen flow rate of 60 mL/min. Ultraviolet-visible (UV–Vis) and fluorescence spectra were measured on a Shimadzu UV-3100 spectrophotometer and Shimadzu RF-5301PC florescence spectrophotometer, respectively. Cyclic voltammetry (CV) was performed on an Autolab Electrochemical Analyzer (ECO Chemie, The Netherlands) system with a three-microelectrode cell (using a platinum working electrode, a Pt wire counter electrode, and a Ag/AgCl reference electrode coated with a film of MPS-PPV and solid electrolyte mixture) at a scan rate of 20 mV/s. The solid electrolyte was a mixture of $LiClO_4$ (20 wt %) and PEO. Current density–voltage (*J–V*) characteristics were tested on EG and PARC M273 electrochemical analysis system. The two electrodes were shorted together for 200 s before a measurement to discharge the capacitor and ensure that steady state had been reached. The morphology via atomic force microscope (AFM) was obtained by Nano Scope III a.

Fabrication and characterization of lec devices

Cleaning of the ITO includes ultrasonication and extraction steps in $CHCl_3$ and ethanol. The fabrication of the SLEC was carried out as follows: MPS-PPV (0.10 g) was dissolved in a mixture of acetone (2.0 mL) and distilled water (3.0 mL). The filtered solution was spin-coated (2000 rpm) onto the ITO substrate (sheet resistance about 50 Ω/ □). The obtained film was dried in a vacuum oven for 24 h. The aluminum contact (about 500 nm in thickness) was deposited onto the active luminescent polymer layer by vacuum evaporation (1×10^{-6} Torr). The active area of the electroluminescent devices was approximately 0.25 cm^2.

Synthesis

5-Methoxy-2-(3-sulfonatopropoxy)-1,4-xylene α,α′-dichloride (2)

Potassium 3-(4-methoxyphenoxy)propanesulfonate(1) was obtained by the reaction of potassium 4-methoxy phenoxide with 1,3-propanesultone in anhydrous ethanol (yield, 90%). To a stirred solution of **1** (3.0 g, 7.86 mmol) in 22 mL of water and 9 mL of concentrated hydrochloric acid, cooled to 2°C, 11 mL of 37% formalin solution was added. A stream of hydrogen chloride gas was bubbled through the mixture for 30 min, and then the temperature was increased to 40°C. The mixture was saturated with hydrogen chloride throughout, and the reaction was stopped until white turbid liquid was observed. After centrifugation, the solvents were completely removed to give a gray-white residue, and then washed by methanol for three times. Elimination of the solvent and drying in a vacuum oven afforded a gray-white solid compound **2** (3.1 g; yield, 60%).^{1}H NMR (*d*-DMSO) δ (ppm): 1.9–2.1 (2H, —CC**H**$_2$C—, m), 2.5–2.7 (2H, —C**H**$_2$—SO_3, t), 3.6–3.8

(3H, —O—C**H**$_3$, s), 3.9–4.1 (2H, —O—C**H**$_2$—, t), 4.5–4.7 (—C**H**$_2$—Ar, 4H, d), 6.9–7.1 (2H, —C$_6$**H**$_2$—, m); IR (KBr) ν_{max} (cm^{-1}): 3420 (s), 2940 (m), 1640 (m), 1510 (m), 1470 (m), 1410 (m), 1210 (s), 1040 (s), 935 (w), 880 (w), 800 (w), 730 (w), 700 (w), 610 (m), 520 (m).

Poly{[2-methoxy-5-(3-sulfonatopropoxy)-1,4-phenylene]-1,2-ethenediyl}(3)

MPS-PPV can be obtained by Wessling sulfomium precursor.[24,25] Here it was synthesized by Gilch dehydrohalogenation polymerization[26–27] (Scheme 1). 0.8 g (2.33 mmol) of compound **2** was dissolved in a mixture of anhydrous *tert*-butanol (5 mL) and THF (20 mL) in a 100-mL dried round bottomed flask, which was equipped with a magnetic stirring bar and capped with a rubber septum. A solution of potassium *tert*-butoxide (1.00 g, 8.92 mmol) in anhydrous *tert*-butanol (5 mL) was added dropwise to the reaction flask via a syringe at room temperature. The reaction mixture turned from yellow to orange with the addition of potassium *tert*-butoxide. The reaction mixture was stirred for another 24 h at room temperature after the completion of the addition. The resulting polymer was precipitated from methanol and collected by centrifugation. After drying under a vacuum oven for 24 h, orange powder **3** (0.75 g) was obtained in 95% yield. ^{1}H NMR (D_2O) δ (ppm): 1.7–2.2 (2H, —CC**H**$_2$C—, m), 2.6–3.2 (2H, —C**H**$_2$—SO_3, m), 3.3–4.2 (5H, —O—C**H**$_3$, —O—C**H**$_2$—, m), 5.4–7.4 (4H, —**H**C═C**H**—, —C$_6$**H**$_2$—, m); IR (KBr) ν_{max} (cm^{-1}): 3448 (m), 3060 (w), 2936 (m), 1630 (w), 1577 (m), 1505 (m), 1465 (w), 1411 (m), 1206 (s), 1042 (s), 970 (w), 922 (w), 872 (w), 795 (w), 737 (w), 614 (m), 530 (m). Calcd. for $C_{12}H_{13}KO_5S$ (Mol. Wt. monomeric unit: 308.39): C, 46.74; H, 4.25; S, 10.40; K, 12.68%. Found: C, 41.76; H, 4.62; S, 10.09; K, 12.90%. GPC analysis revealed that the number average molecular weight (M_n) and weight average molecular weight (M_w) of the polymer are 13,700 and 24,000 with a polydispersity index of 1.75. The IR spectrum shows the presence of olefins. The peak at 3060 cm^{-1} corresponds to the C—H stretching vibration mode of olefin, and the peaks at 970 and 737 cm^{-1} are attributed to the C—H bending vibrations of the *trans*- and *cis*-olefins, respectively.

RESULTS AND DISCUSSION

Optical absorption and emission spectra

UV–Vis absorption and photo-luminescent (PL) spectra for MPS-PPV are depicted in Figure 1. MPS-PPV shows optical absorption at 425 nm and 295 nm. These peaks arise from π-electron transitions from delocalized occupied molecular orbitals to delocalized unoccupied ones.[28] The magnitude of the energy gap in PPV is approximately 2.5 eV. The edge absorption of

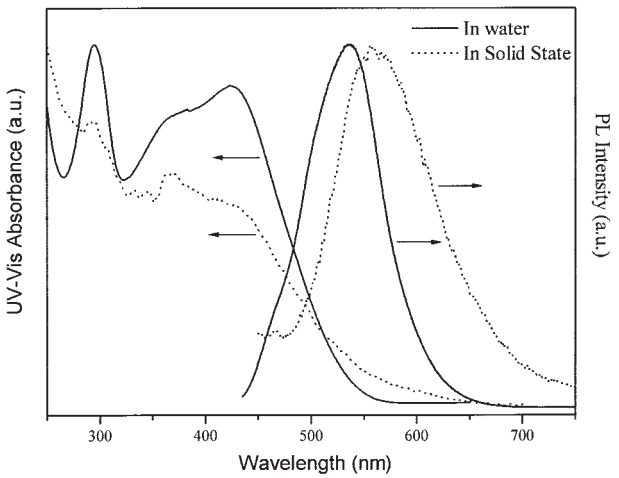

Figure 1 UV–vis absorption and PL spectra of the MPS-PPV in solid state (dash line) or water (solid line).

MPS-PPV in aqueous solution is at 540 nm, corresponding to an optical band gap of 2.30 eV. MPS-PPV show typical behavior of polyelectrolyte, that is, electrostatic repulsion between anionic side-groups dissociated in water results in a rod-like conformation with a persistence length much larger than that of PPV in organic solvent. It is notable that edge absorption of MPS-PPV in the solid-state moves to 610 nm (band gap of 2.04 eV), which implies that the conformation in the membrane is in a rather ordered state. Once MPS-PPV molecule in water is excited by the absorption of a photon with wavelength of 425 nm, it returns to the ground state by emission of green light with maximum wavelength of 535 nm (Fig. 1).

Band structure of MPS-PPV

Besides luminescent properties, electron and hole injection ability of conjugated polymer sandwiched between two electrodes is also critical for performance of electroluminescent devices. Figure 2 depicts the cyclic voltammogram of MPS-PPV. The onset potentials of the reduction and oxidation are −0.83 V and 1.04 V versus Ag/AgCl reference electrode, respectively. According to the standard normal potential (0.24 V) of ferrocene/ferrocenium in this system and its vacuum energy level (4.8 eV)[29], the highest occupied molecular orbital and lowest unoccupied molecular orbital energy levels of the material are estimated to be 5.60 and 3.73 eV, respectively. The energy gap is 1.87 eV, which is approximate to the band gap obtained by electronic spectra. Hole and electron transport states of PPV are located at 5.35 and 2.12 eV, respectively, (Fig. 3). The work function of the ITO electrode amount to 4.8 eV (and 4.2 eV for Al electrode). The contact barrier for electron injection from Al electrode to MPS-PPV is 0.47 eV, much lower than that of PPV (2.08 eV), which

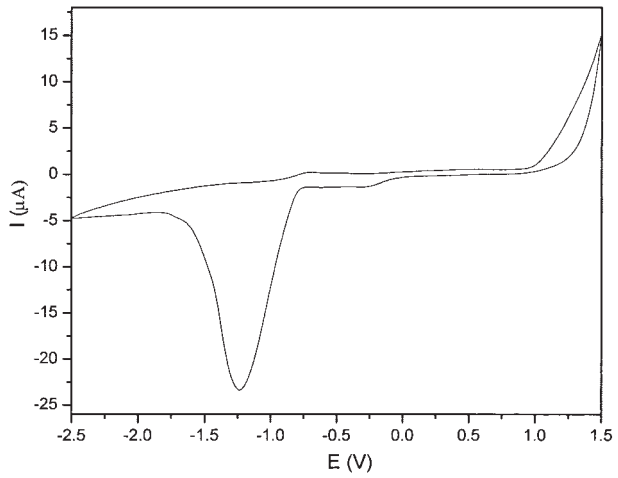

Figure 2 Cyclic voltammogram of MPS-PPV/PEO/$LiClO_4$ at a scan rate of 20 mV/s; Ag wires were used as reference electrode.

indicates that the electron injection ability of conjugated polymer can be greatly improved through incorporation of ionic species into the backbone. When MPS-PPV is used as the active layer, a better performance of the device would be expected owing to reduced contact barrier and more balanced injection of hole and electron.

Morphology

Figure 4 shows the atomic force microscopy (AFM) image of the spin-coated film of MPS-PPV onto ITO glass. The topographic image of the film that is vacuum-dried at room temperature exhibits very smooth surface morphology with a root mean square (RMS) value of 0.397 nm. Therefore, there is no obvious phase separation in luminescent active layer, as expected.

Dual electroluminescent and *J–V* characteristics of single-component LEC

The single-component LEC device that we fabricate has a sandwich configuration of ITO/MPS-PPV/Al. Dependence of current density (J) and EL intensity on operation voltage (V) are displayed in Figure 5. Single-layer light-emitting devices based on ordinary PPV and its derivatives show typical characteristics of semiconductor, i.e., a onset of current at high forward (positive) bias and extremely weak current under reverse (negative) bias. The apparent threshold voltage for detection of EL under forward bias is usually more than 10 V. Moreover, no light emission is detectable under reverse bias. Although the structure of our device is identical to traditional single-layer LEDs, it is interesting that the electroluminescent and *J–V* characteristic is quite similar to LECs consisting of a blend of conjugated luminescent polymers and solid electrolyte along with lithium salt. Our device can be operated in both forward and reverse bias (Fig. 5). Dual EL is observed under ambient conditions. Figure 6 describes the EL spectra recorded under forward and reverse bias with the same magnitude (±8V). They all display an emission band with the maximum around 520 nm, which corresponds to green light. The peak is blue-shifted about 40 nm with respect to the PL spectrum of a solid film. It is also notable that the apparent threshold voltage for the detection of light emission is rather low (+4 V and −5 V). In addition, the forward onset of the current is around +3 V (−4 V for reverse operation).

The distinct behavior of current device can be explained as follows. In luminescent active layer, anions (SO_3^-) covalently attached to the conjugated chains and cations (K^+) disperse homogeneously over the whole layer (Fig. 7(a)). With the aid of external electric field, dissociated cations move toward and accumulate near the cathode to form Ohmic contact between MPS-PPV and electrode (Fig. 7(b)). Low turn-on voltage arises from the reduction of the contact barrier to electron carrier injection.

Slightly asymmetrical *J–V* can be observed in our device (Fig. 5). Rectification ratio (ratio of forward to reverse current at a certain applied voltage) ranges between 1.3 and 1.9 (unity for symmetric LEC). Meanwhile the "reverse" emission is slightly weaker than the "forward" emission (Fig. 6). All these behavior may be associated with fact that the migration of anionic toward anode (Al) under reverse bias is rather difficult, which leads to larger barrier heights for hole

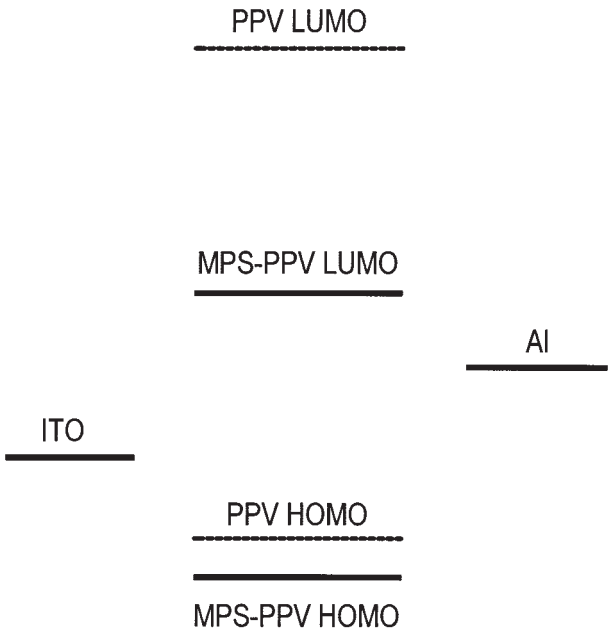

Figure 3 Schematic diagram indicating the band structure of PPVs and the work function of the electrodes.

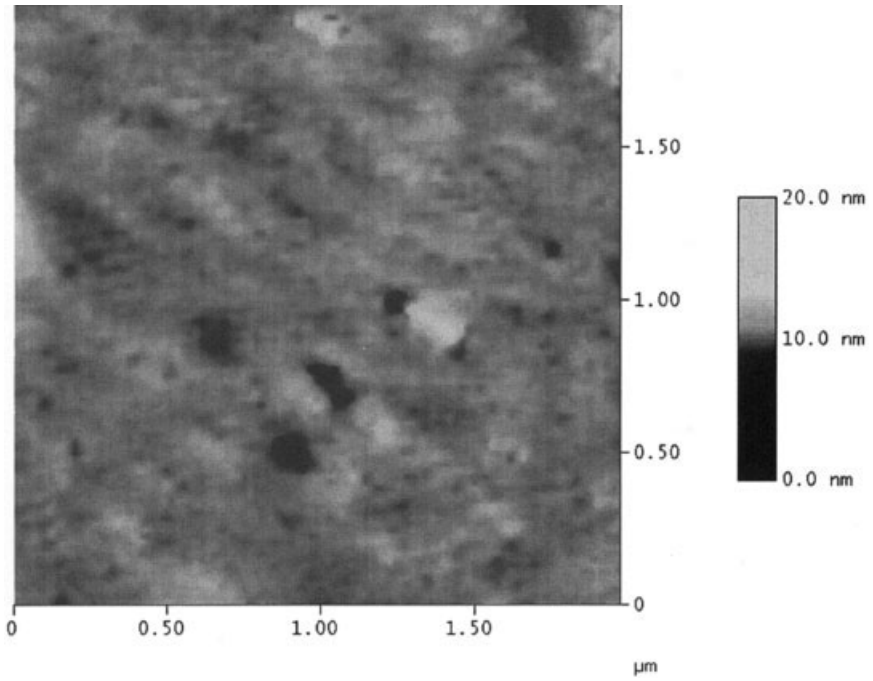

Figure 4 Atomic force microscopy image of the MPS-PPV film spin-coated onto ITO glass.

injection and a mismatch in the injection rate of electrons and holes that limits the EL efficiency.

Stability of electroluminescent material and devices

Thermogravimetric analysis is shown in Figure 8. MPS-PPV exhibits an onset of degradation at 330°C, while the maximum rate of weight loss takes place at temperature above 350°C. The result reveals that this material shows favorable thermal stabilities in nitrogen atmosphere, which may be appropriate for long-life operation of electroluminescent device.

Figure 9 displays the time response of current and luminance for the device biased at +6.0 V. The stable current and light-emission indicate that the single-component device could sustain long-term operations without much loss of efficiency (around 85% of its original reading). Since the fabrication and characterization of the devices were conducted under ambient conditions, better EL performance may be expected if the processing is carried out in more strict conditions.

No breakdown of our device was found with operating voltage up to 16 V. This indicates the stability of our device at high voltage.

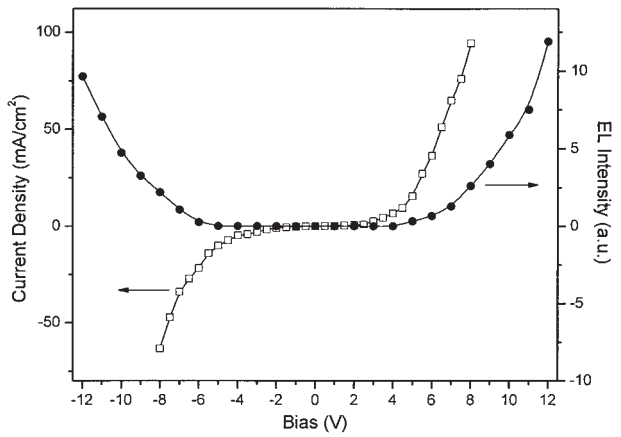

Figure 5 The current density–voltage (-□-) and EL intensity–voltage (-●-) characteristics of the ITO/MPS-PPV/Al device.

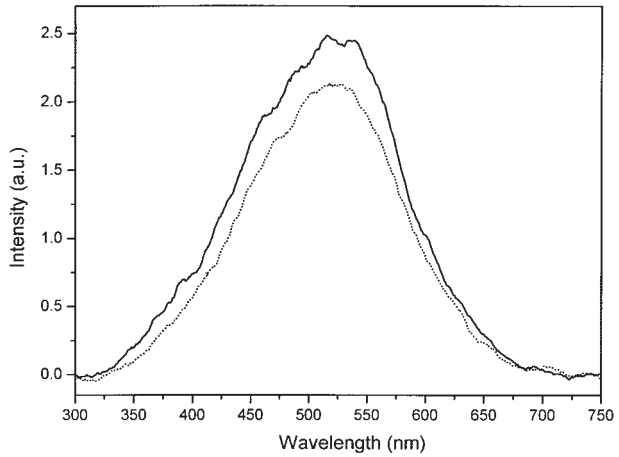

Figure 6 Electroluminescent spectra of the ITO/MPS-PPV/Al device under forward (solid line) and reverse (dash line) bias of 8 V.

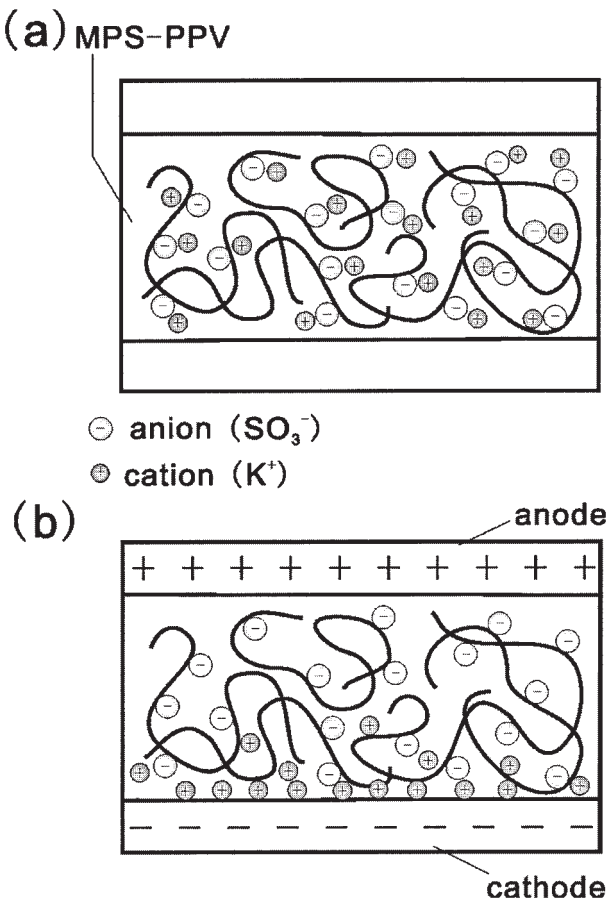

Figure 7 Distribution of the ionic species in the ITO/MPS-PPV/Al device before (a) and after (b) the application of external electric field.

CONCLUSIONS

We investigate an anionic water-soluble conjugated polymer having "green" or environmentally benign characteristics. MPS-PPV serves as both electronic and ionic conductor and is an ideal material for construction of single-component electroluminescent devices with low turn-on voltage, dual light-emission under both forward and reverse bias, and stability when operated under ambient conditions. Our research opens up a wide field for further investigation into water-soluble conjugated polymers in EL application.

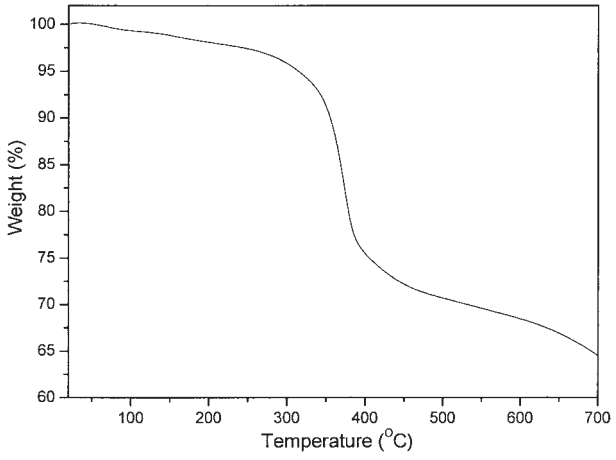

Figure 8 TGA thermograms of the MPS-PPV.

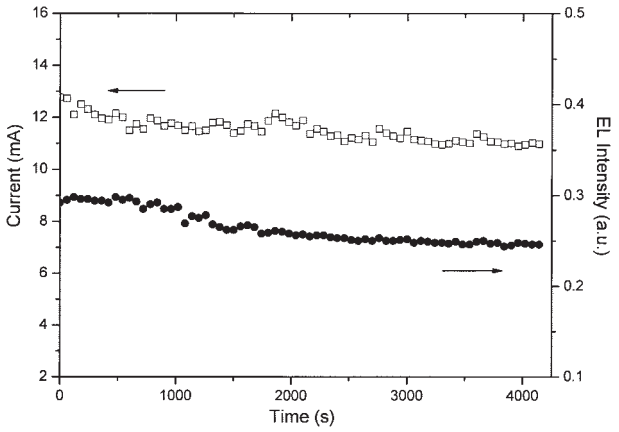

Figure 9 Time response of current (□) and luminance (●) for the ITO/MPS-PPV/Al device under forward bias (+6.0 V).

The authors thank Professor Mu Wang at National Laboratory of Solid State Microstructures, Nanjing University, for providing AFM, used in this investigation.

References

1. Burroughes, J. H.; Bradley, D. D. C.; Brown, A. R.; Marks, R. N.; Mackay, K.; Friend, R. H.; Burns, P. L.; Holmes, A. B. Nature 1990, 347, 539.
2. Pei, Q. B.; Yu, G.; Zhang, C.; Yang, Y.; Heeger A. J Science 1995, 269, 1086.
3. Pei, Q.; Yang, Y.; Yu, G.; Zhang, C.; Heeger, A. J. J Am Chem Soc 1996, 118, 3922.
4. deMello, J. C.; Tessler, N.; Graham, S. C.; Friend, R. H. Phys Rev B 1998, 57, 12951.
5. deMello, J. C. Phys Rev B 2002, 66, 235210.
6. Cao, Y.; Yu, G.; Heeger, A. J.; Yang, C. Y. Appl Phys Lett 1996, 68, 3218.
7. Yu, G.; Cao, Y.; Zhang, C.; Li, Y.; Gao, J; Heeger, A. J. Appl Phys Lett 1998, 73, 111.
8. Campbell, I. H.; Smith, D. L. Appl Phys Lett 1998, 72, 2565.
9. Edman, L.; Summers, M. A.; Buratto, S. K.; Heeger, A. J.; Phys Rev B 2004, 70, 115212.
10. Morgado, J; Cacialli, F.; Friend, R. H.; Chuah, B. S.; Rost, H.; Holmes, A. B.; Macromolecules 2001, 34, 3094.
11. Yang, C.; Sun, Q.; Qiao, J.; Li, Y. J Phys Chem B 2003, 107, 12981.
12. Chuah, B. S.; Hwang, D.-H.; Kim, S. T.; Moratti, S. C.; Holmes, A. B.; De Mello, J. C.; Friend, R. H. Synth Met 1997, 91, 279.
13. Winkler, B.; Dai, L.; Mau, A. W.-H. Chem Mater 1999, 11, 704.
14. Xiang, D.; Shen, Q. D.; Zhang, S.; Jiang X. J Appl Polym Sci 2003, 88, 1350.
15. Yin, C.; Zhao, Y. Z.; Yang, C. Z.; Zhang, S. Y. Chem Mater 2000, 12, 1853.

16. Heeger, P. S.; Heeger, A. J Proc Natl Acad Sci USA 1999, 96, 12219.
17. Chen, L.; McBranch, D. W.; Wang, H. L.; Helgeson, R.; Wudl, F.; Whitten, D. G. Proc Natl Acad Sci USA 1999, 96, 12287.
18. Liu, B.; Gaylord, B. S.; Wang, S.; Bazan, G. C. J Am Chem Soc 2003, 125, 6705.
19. Wang, S.; Bazan, G. C. Adv Mater 2003, 15, 1425.
20. Xu, Q. H.; Gaylord, B. S.; Wang, S.; Bazan, G. C.; Moses, D.; Heeger, A. J Proc Natl Acad Sci USA 2004, 101, 11634.
21. Gaylord, B. S.; Massie, M. R.; Feinstein, S. C.; Bazan, G. C. Proc Natl Acad Sci USA 2005, 102, 34.
22. Sirringhaus, H.; Kawase, T.; Friend, R. H.; Shirmoda T.; Inbasekaran M.; Wu, W.; Woo, E. P.; Science 2000, 290, 2123.
23. Chang, S.; Bharathan, J.; Yang, Y.; Helgeson, R.; Wudl, F.; Ramey, M. B.; Reynolds, J. R. Appl Phys Lett 1998, 73, 2561.
24. Shi, S.; Wudl, F. Macromolecules 1990, 23, 2119.
25. Wang, D. Ph. D. Thesis (Univ. of California, Santa Barbara), 2001.
26. Wudl, F.; Hoger, S.; Zhang, C.; Pakbaz, K.; Heeger, A. J Polym Prepr 1993, 34, 197.
27. Dalvi-Malhotra, J.; Chen, L. J Phys Chem B 2005, 109, 3873.
28. Kohler, A.; dos Santos, D. A.; Beljonne, D.; Shuai, Z.; Bredas, J.-L.; Holmes, A. B.; Kraus, A.; Mullen, K.; Friend, R. H. Nature 1998, 392, 903.
29. Pasco, S. T.; Lahti, P. M.; Karasz, F. E. Macromolecules 1999, 32, 6933.